Universal afterglow of supernovaless gamma-ray bursts

Shlomo Dado and Arnon Dar
Physics Department, Technion, Haifa 32000, Israel

(Received 23 July 2018; revised manuscript received 13 February 2019; published 28 June 2019)

The early-time afterglows of gamma-ray bursts (GRBs) not associated with a supernova (SN) explosion (SN-less GRBs) can be scaled down to a dimensionless, parameter-free universal behavior. This universal behavior is that expected from a pulsar wind nebula afterglow powered by the rotational energy loss of a newly born pulsar. Such SN-less GRBs include short-hard bursts produced by the merger of binary neutron stars and long bursts presumably produced by the accretion-induced collapse of neutron stars to quark stars in high-mass x-ray binaries, or in isolation due to energy and angular momentum loss.

DOI: 10.1103/PhysRevD.99.123031

I. INTRODUCTION

Gamma-ray bursts (GRBs) are brief flashes of gamma rays lasting between a few milliseconds and several hours [1] from extremely energetic cosmic explosions [2]. They were first detected in 1967 by the Vela satellites. Their discovery was published in 1973 after 15 such events were detected [3]. GRBs fall roughly into two classes [4]: long-duration ones (LGRBs) that last more than ∼2 seconds, and short-hard bursts (SGRBs) that typically last less than 2 seconds. For three decades after their discovery, the origin of both types was completely unknown. This has changed dramatically with the first x-ray localization of GRBs and the discovery of their x-ray afterglow with the BeppoSAX satellite, which led also to the discovery of GRBs' afterglow at longer wavelengths, their host galaxies and their redshifts [5], and to the detailed measurements with ground- and space-based telescopes of the properties of their prompt and afterglow emissions, their host galaxies, and their nearby environments.

The late-time afterglow of GRB970228, the first localized GRB observed by BeppoSAX, also included photometric evidence of an associated supernova [6] which met skepticism, as did [7] the original suggestions of a GRB-supernova (SN) association [8] long before this first observational evidence. It was only after photometric and spectroscopic evidence [9] for other SN-LGRB associations was accumulated from relatively nearby LGRBs that the SN-LGRB association was widely accepted. Moreover, it was also believed (e.g., Ref. [10]) that type Ic supernovae (SNIc) (akin to 1998bw) were not observed in ordinary LGRBs because they were too distant, they were outshined by the GRB afterglow and/or the light of the host galaxy, or that they simply were not looked for. However, deep optical searches of SNe associated with several relatively nearby LGRBs have failed to detect an associated SN [11]. They provided compelling evidence that SN explosions are not the only source of LGRBs. But their origin has not been established beyond doubt and is still debated.

As for SGRBs, until recently they were widely believed to be produced in neutron star mergers in compact neutron star binaries [12] following gravitational-wave emission, as was first suggested three decades ago [13], and perhaps in neutron star–black hole mergers [14]. This wide belief was based on indirect evidence [12]. Recently, however, the short-hard burst SHB170817A that followed ∼1.7 s after GW170817 [15], the first direct detection of gravitational waves (GWs) emitted from a neutron star merger, by the LIGO-Virgo GW detectors [16], has shown beyond a doubt that neutron star mergers produce SGRBs.

In this paper, we show that all the well-sampled x-ray afterglows of SN-less GRBs within the first couple of days after the burst have a temporal behavior, which can be scaled down to a simple dimensionless universal form. This universal form is expected if the afterglows of SGRBs and SN-less LGRBs during the first couple of days after the burst are dominated by the emission of a pulsar wind nebula (PWN) powered by the newly born pulsar [17]. Several implications of these observations are briefly discussed.

II. UNIVERSAL AFTERGLOWS

As long as the spin down of a pulsar with a period $P(t)$ satisfies $\dot{P}P = \text{const}$,

$$P(t) = P_i(1 + t/t_b)^{1/2}, \tag{1}$$

where $P_i = P(0)$ is the initial period of the pulsar, t is the time after its birth, and $t_b = P_i/2\dot{P}_i$. If a constant fraction η of the rotational energy loss of such a pulsar is reradiated by the PWN, then, in a steady state, its luminosity satisfies $L = \eta I w\dot{w}$, where $w = 2\pi/P$ and I is the moment of inertia of the neutron star. Hence, in a steady state, the luminosity emitted by a PWN satisfies

$$L(t) = L(0)/(1 + t/t_b)^2. \quad (2)$$

Equation (2) can be written as

$$L(t)/L(0) = 1/(1 + t_s)^2, \quad (3)$$

where $t_s = t/t_b$. Thus, the dimensionless luminosity $L(t)/L(0)$ has a simple universal form as a function of the scaled time t_s. For each afterglow of an SN-less GRB powered by a pulsar, $L(0)$ and t_b can be obtained from a best fit of Eq. (2) to the light curve of their measured afterglow.

The initial period of the pulsar enshrouded within a PWN can be estimated from its locally measured energy flux $F(0)$ corrected for absorption along the line of sight to the PWN, its redshift z, and its luminosity distance D_L,

$$P_i = \frac{1}{D_L}\sqrt{\frac{(1+z)\eta\pi I}{2F(0)t_b}}, \quad (4)$$

where $F = L/4\pi D_L^2$, $I \approx (2/5)MR^2 \approx 1.12 \times 10^{45}$ g cm^2, for a canonical pulsar with $R = 10$ km and $M \approx 1.4\ M_\odot$, and $\eta < 1$. The period derivative can be obtained from the relation $\dot{P}_i = P_i/2t_b$.

III. COMPARISON WITH OBSERVATIONS

In Ref. [18], we fit the x-ray light curves of all SGRBs with a well-sampled afterglow measured with Swift-XRT [19], assuming the cannonball model for the prompt and extended emission and Eq. (2) for the following afterglow. Figure 1 demonstrates such a fit for SHB150424A.

Equations (2) and (3) are expected to be valid only after the last accretion episode on the newly born pulsar, and after the PWN emission powered by the pulsar has reached a steady state. Since the exact times of both are not known, and in order to avoid a contribution from the prompt emission, we fit the observed afterglows of SN-less GRBs with Eq. (2) after the extrapolated contribution of the fast declining prompt emission to the plateau phase of the prompt emission (last pulse/flare or extended emission) became negligible, i.e., less than the errors of the first data points of the plateau. This, probably, made unimportant the lack of knowledge of the exact birth time/power supply of the pulsar and when the PWN emission powered by the pulsar's power supply had reached a steady state.

In Fig. 2 we plot the dimensionless x-ray afterglow of 12 SGRBs with the best sampled afterglows measured with Swift-XRT [20] in the first couple of days after the burst and the universal behavior given by Eq. (3). In Table I, we list the values of $L(0)$ and t_b used to reduce each measured light curve to the dimensionless universal form. They were obtained for each SGRB from a best fit (minimal χ^2/d.o.f.) of Eq. (2) to the observed plateau plus the fast-decline phase of the x-ray afterglow.

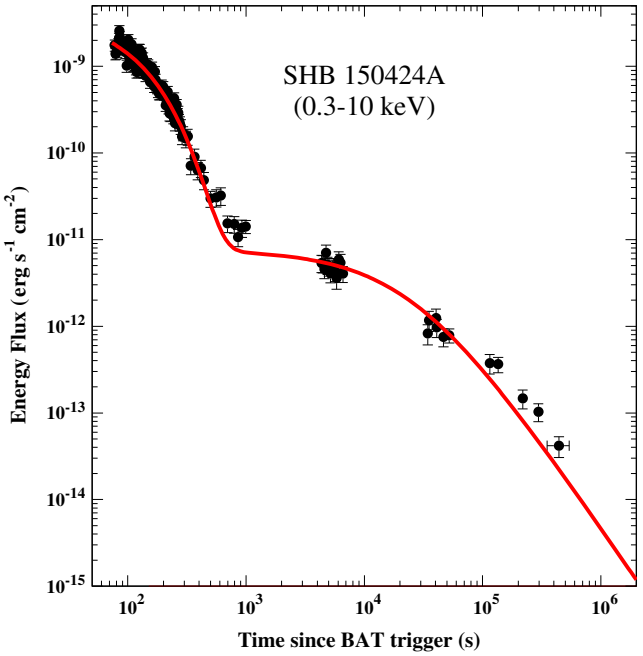

FIG. 1. Comparison between the observed x-ray afterglow of SHB150424A measured with Swift-XRT [19] and the best fit assuming the cannonball model for the prompt and extended emission [18] and Eq. (2) for their late-time afterglow.

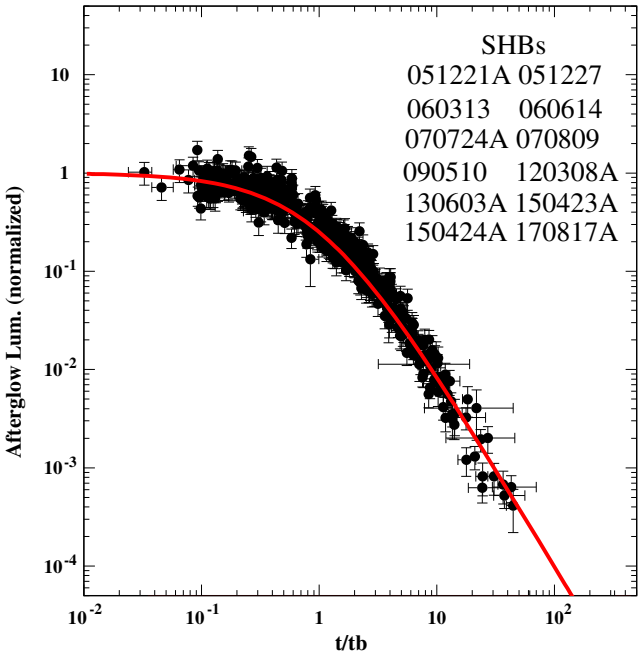

FIG. 2. Comparison between the scaled light curves of the well-sampled x-ray afterglow of 12 SGRBs measured with Swift-XRT [19] during the first couple of days after the burst and their universal behavior predicted by Eq. (3). The bolometric light curve of SHB170817A reported in Ref. [20] is also included. χ^2/d.o.f. $= 761/534 = 1.43$.

TABLE I. Physical parameters extracted from the afterglow of 13 SGRBs.

SHB	z	$F_X(0)$ [erg/s cm^2]	t_b [s]	χ^2/ d.o.f.	$P_i/\sqrt{\eta}$ [ms]
051221A	0.5465	2.33E-12	46276	1.04	16.2
051227	0.8	1.44E-11	2280	0.93	19.8
060313		2.91E-11	4482	0.60	
060614	0.125	1.41E-11	41733	1.39	33.2
061201	0.111	1.34E-10	1343	1.23	65.4
070724A	0.457	1.18E-12	18041	1.47	43.7
070809	0.2187	3.231E-12	17181	1.05	57.6
090510	0.903	3.68E-10	551	1.76	7.04
120308A		6.84E-11	4742	1.67	
130603B	0.3564	6.00E-11	3578	1.29	17.8
150423A	1.394	1.31E-11	1290	1.36	16.0
150424A	0.30	6.1E-12	31805	1.24	22.4
170817A	0.0093		117344	0.60	

The predicted universal behavior of the afterglow of SN-less LGRBs as given by Eq. (2) is compared in Fig. 3 to the observed light curves of the afterglows of the long-duration GRB990510, in the x-ray [21] and optical I, R, V, B bands [22], scaled according to Eq. (3) and plotted as a function of t/t_b.

Unlike SGRBs which seem to be produced by the merger of neutron stars in binary neutron stars, LGRBs seem to consist of two main classes [23]: SN-LGRBs and SN-less LGRBs. Only in relatively nearby long GRBs could the GRB class be identified using deep photometric and spectroscopic searches of an associated SN. However, SN-LGRBs are produced mostly in star formation regions within molecular clouds of relatively high density. In such cases, the LGRB afterglow seems to be dominated by the synchrotron radiation emitted from a decelerating highly relativistic jet in the dense interstellar medium (ISM). The spectral energy density of their emitted afterglow is well described by a smoothly broken power law with a spectral index β and a temporal decay index α which well after the "break" satisfies the closure relation $\alpha = \beta + 1/2$ predicted by the cannonball (CB) model of SN-LGRBs [24]. This relation seems to be well satisfied by SN-LGRBs but not by SN-less LGRBs. In more distant LGRBs, where an SN-LGRB association could not be established because the SN could have been outshined by the GRB afterglow and/or by the host galaxy, or simply was not looked for, the above closure relation was used to identify a potential SN-LGRBs identity whose afterglow was produced by synchrotron emission from a decelerating highly relativistic jet [25].

The well-sampled afterglows of a representative set of five SN-less LGRBs measured with Swift-XRT [19] in 2018 during the first few days after burst are compared in Fig. 4 to their expected universal behavior given by Eq. (3). Different colors represent the light curves of different GRBs. The parameters $L(0)$ and t_b, used to reduce each measured afterglow light curve to the dimensionless universal form,

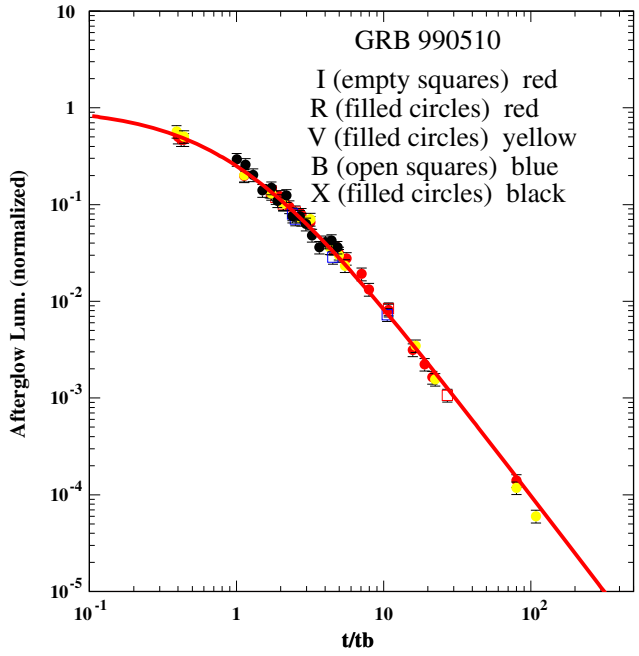

FIG. 3. Comparison between the observed afterglow of GRB990510 in the x-ray [21] and optical I, R, V, B bands [22] scaled according to Eq. (2) and plotted as function of t/t_b, and their predicted universal form as given by Eq. (3), which yields $\chi^2/\text{d.o.f.} = 45.52/54 = 0.84$.

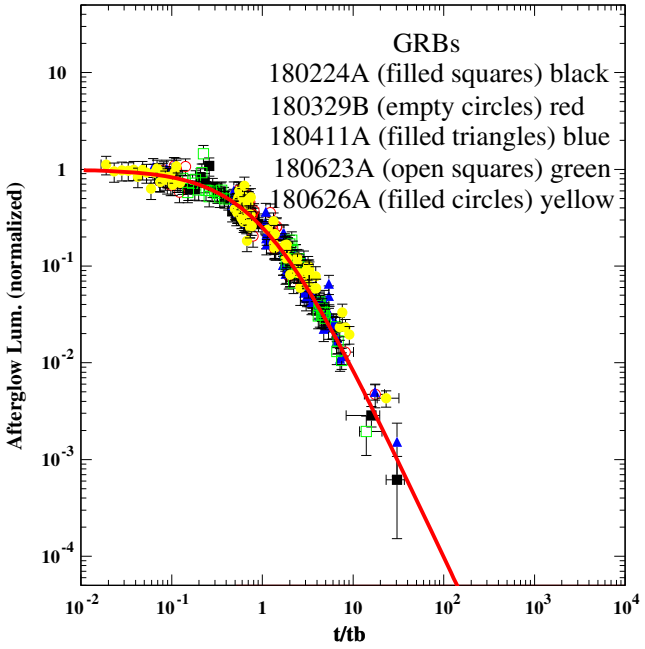

FIG. 4. Comparison between the predicted universal behavior given by Eq. (3) and the reduced x-ray afterglow of five SN-less GRBs with well-sampled x-ray light curves measured in 2018 with Swift-XRT [19] in the first couple of days after the burst, and their predicted universal behavior as given by Eq. (3). $\chi^2/\text{d.o.f.} = 352/339 = 1.04$.

TABLE II. Physical parameters extracted from the afterglow of 43 LGRBs.

GRB	z	$F_X(0)$ [erg/s cm^2]	t_b [s]	χ^2/ d.o.f.	$P_i/\sqrt{\eta}$ [ms]
050318	1.44	1.03E-10	3972	0.92	3.14
050319	3.24	1.56E-11	33136	0.90	1.36
050326		1.50E-10	3138	1.38	
050505	4.27	3.56E-11	14059	0.89	1.12
050713B		1.62E-11	60641	1.28	
051008	2.77	6.03E-11	5865	1.41	1.88
051016B	0.936	2.86E-12	49340	0.84	2.09
060510A		2.35E-10	10695	1.29	
060526	3.221	7.41E-12	19526	1.21	3.22
060605	3.78	4.74E-11	4320	1.35	1.95
061004		9.03E-12	7016	1.08	
061222A	2.088	4.32E-11	29993	1.06	1.20
151027A	0.81	5.42E-10	5522	1.35	
160131A	0.972	7.14E-11	12189	1.61	3.19
160227A	2.38	1.06E-11	95109	1.72	1.29
160509A	1.17	6.23E-11	51257	1.17	1.39
160824A		6.81E-11	8410	0.91	
160905A		1.38E-10	13747	1.27	
161014A	2.823	3.82E-10	1393	1.78	1.57
161017A	2.013	4.77E-11	12231	1.13	2.00
170519A		3.17E-11	10829	1.23	
170711A		3.97E-12	46121	1.38	
170810A		3.07E-11	10657	1.79	
170822A		1.09E-9	1424	1.18	
170903A		4.11E-12	85254	1.49	
170912B		1.55E-10	1393	1.06	
171010A		2.51E-11	66392	0.88	
171102B		3.85E-11	5630	0.80	
171120A		1.67E-11	34899	0.95	
171222A	2.409	8.22E-13	249130	1.13	2.78
180224A		1.02E-10	1537	0.84	
180329B	1.998	2.54E-11	8542	0.94	2.15
180331B		1.03E-11	3833	1.10	
180411A		9.30E-11	9510	0.98	
180425A		1.39E-12	69507	1.23	
180623A		2.17E-10	2498	0.93	
180626A		3.37E-11	9000	1.43	
180818B		2.11E-11	17147	0.99	
181103A		4.78E-12	40532	1.05	
181202A		2.43E-12	31163	1.64	
190106A	1.859	3.85E-11	34916	1.24	1.37
190114A	3.376	2.64E-11	9880	0.88	1.86
190203A		1.43E-9	1662	0.72	

were obtained from a best fit of Eq. (2) to their x-ray afterglow. Their best values are listed in Table II. The number of GRBs in Fig. 4 has been limited to five in order to avoid obscuring the data points by overlying points. The dispersion of the 339 data points around the universal shape yields a very satisfactory $\chi^2/\text{d.o.f.} = 352/339 = 1.04$.

Following Figs. 3 and 4 we have verified that the x-ray light curves of almost all the SN-less GRBs with a well-sampled x-ray afterglow in the first couple of days after the burst that have been measured with the Swift-XRT [19] during the past 15 years after the launch of Swift, i.e., those that show an initial plateau, but are without an identified SN association and do not satisfy the late-time CB model closure relation of SN-LGRBs, seem to satisfy Eqs. (2) and (3) ($\chi^2/\text{d.o.f.} \sim 1$). This is demonstrated in Fig. 5 and in Table II, for the x-ray afterglow of SN-Less LGRBs measured with the SWIFT XRT (19) in the first 1 years (2005, 2006) after the launch of Swift and in the past 5 years (2015–2019).

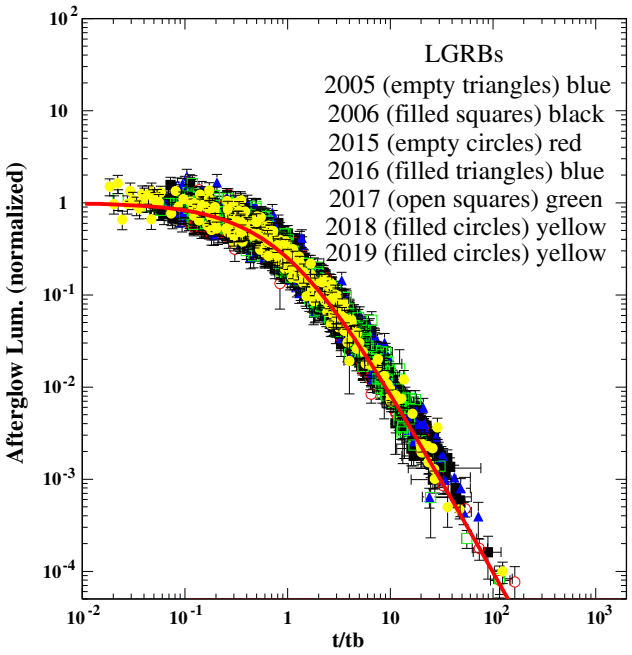

FIG. 5. Comparison between the predicted universal behavior given by Eq. (3) and the reduced light curves of the x-ray afterglow of SN-less GRBs with a well-sampled light curve of their x-ray afterglow measured within a few days after the burst with the SWIFT XRT (19) in the first 2 years (2005, 2006) after launch and in the past 5 years (2015–2019). The different colors indicate data points from different years. The dispersion of the data points has a $\chi^2/\text{d.o.f.} = 3927/3233 = 1.21$.

Tables I and II summarize the parameters in Eq. (2) that best reproduce the x-ray afterglows of the SN-less GRBs shown in Figs. 1–5 and the pulsar periods derived from them using Eq. (4) with $\eta = 1$.

More details on the statistical analysis and the agreement between the observations and the universal behavior of the alight curves of the x-ray afterglow of SN-less GRBs are included in the Appendix.

Although, most of the data points in Fig. 5 are obscured by overlying points from later years, the colors indicate a decreasing dispersion in recent years of data points around the predicted universal behavior. It is probably due to increasing measurement accuracy in recent years. In order to demonstrate that, we have separated in the Appendix the comparison of the data included in Fig. 5 and the predicted

universal behavior, into comparisons in individual years, shown in Figs. 6–9. Note that the value of the χ^2/d.o.f. statistic has decreased as a function of time from 1.35 in 2015–2016 to 1.25 in 2017 and to 1.02 in 2018–2019.

IV. DISCUSSION AND CONCLUSIONS

All the well-sampled afterglows of SGRBs within a few days after the burst seem to be well described by Eqs. (2) and (3) as shown in Figs. 1 and 2. That, and the detection of SHB170817A [15], which followed the detection of GWs from GW170817 by the Virgo-Ligo GW detector [16], indicates that SGRBs are produced mainly by neutron star mergers [13] and not by neutron star–black hole mergers [14] in compact binaries.

LGRBs seem to consist of two distinct populations: SN-less LGRBs and SN-LGRBs. An SN-less identity was established observationally only for relatively nearby LGRBs by very deep searches [11]. In more distant LGRBs, an SN-less identity could not be established because the SN could have been outshined by the GRB afterglow and/or the host galaxy, or simply was not looked for.

An indirect way of identifying SN-less LGRBs is the characteristic universal afterglow of SN-less LGRBs, which is very different from the afterglow of SN-LGRBs: the late-time afterglow of SN-LGRBs seems to have a spectral energy flux density, which is well described by $F_\nu \propto t^{-\alpha}\nu^{-\beta}$ with $\alpha = \beta + 1/2$, as predicted [24] by the CB model of SN-LGRBs, where a highly relativistic jet of CBs ejected in an SNIc explosion produces the afterglow by synchrotron radiation emitted during their deceleration in the ISM.

The afterglow of SN-less LGRBs seems to be quite different. It has the simple temporal behavior of an isotropic afterglow well described by Eq. (2) within the first few days after the burst, and can be scaled down to the universal behavior given by Eq. (3). This is demonstrated in Fig. 3 for GRB990510 and in Figs. 2 and 4–9 for SN-less LGRBs with well-sampled x-ray afterglows during the first couple of days after the burst, measured with Swift-XRT [19] in the first 2 years (2005, 2006) after launch and in the past 5 years (2015–2019). Hence, the early claims in Refs. [21] and [22] of beamed afterglow emission from GRB 990510 and in many following publications on the afterglow of other SN-less GRBs, which were based on arbitrary parametrizations or heuristic functions, rather than on properly derived functions from an underlying jet model, apparently were premature and mistaken.

Figures 2–9 clearly demonstrate that although the relation $\dot{P}P = \text{const}$ has been derived [26] for pulsars which spin down by magnetic dipole radiation (MDR) (in vacuum and assuming a time-independent magnetic field and moment of inertia during the spin down), the GRB data suggests that it may be more general. For instance, it is satisfied to a good accuracy by the Crab pulsar, despite the fact that the total luminosity of the Crab PWN which is powered by the Crab pulsar, is much higher than its MDR luminosity, estimated from its current P and $\dot{P}$. The PWN can be powered by pulsar cosmic-ray particles and relativistic winds.

Indeed, relativistic wind (RW) particles and high-energy cosmic rays (CRs) with $E \approx pc$, which spiral out along the open magnetic field lines and escape at the light cylinder (of a radius c/w around the rotation axis) carry out energy E and angular momentum l at a rate $\dot{E} = \text{Lum(CR)} + \text{Lum(RW)}$ and $\dot{l} = I\dot{w} = \text{Lum}/w$, respectively, where $\text{Lum} = \text{Lum(CR)} + \text{Lum(RW)}$ is the energy loss rate by CRs and RW. If this loss of angular momentum dominates the spin down of a pulsar, then the estimate [26] of its magnetic field at the magnetic poles, $B_p = 6.4 \times 10^{19}\sqrt{P\dot{P}}$ Gauss, is an overestimate. Moreover, this estimate assumes a vacuum environment and a time-independent magnetic field [26] for the newly born millisecond pulsar (MSP), and cannot be trusted as solid evidence that MSPs which seem to power the afterglows of SN-less LGRBs are magnetars [27].

If the afterglow of SN-less GRBs is powered by a newly born MSP, then the period which is obtained from best fits of Eq. (2) to its afterglow must yield periods well above the classical Newtonian lower limit $P > 2\pi R/c \approx 0.2$ ms for canonical neutron stars. So far, all the fitted SN-less GRBs have yielded much larger periods than 0.2 ms. However, if the early-time energy flux from the newly born pulsars is much larger than that of the afterglow measured by Swift-XRT in the 0.3–10 keV range then the periods listed in Tables I and II are actually upper bounds.

It is, however, quite remarkable that the inferred periods of the newly born pulsars in SGRBs are typically an order of magnitude longer than those inferred for SN-less LGRBs. That may be due to the efficient removal of angular momentum by gravitational wave emission in neutron-star mergers compared to the spin up of neutron stars in high-mass x-ray binaries, or in the collapse of solitary neutron stars to the more compact quark stars following energy and angular momentum loss. It may also indicate that the transfer of rotational energy from the collapsing core to outer layers in core-collapse SN explosions, which is needed to keep its surface velocity below the speed of light, may play an important role in core-collapse SN explosions. Such a transfer of rotational energy to the stellar envelope may help neutrinos and shock waves from a core collapse blow up the stellar envelope, which so far alone could not produce consistently (in numerical simulations) core-collapse SN explosions of massive stars with kinetic energy $E_k \gtrsim 10^{51}$ erg [28].

ACKNOWLEDGMENTS

The authors thank Erez Ribak and an anonymous referee for very useful suggestions.

APPENDIX: ADDITIONAL INFORMATION ON THE STATISTICAL ANALYSIS

The best-fit values of the parameters t_b and $L(0)$ for each GRB reported in Tables I and II, were obtained with

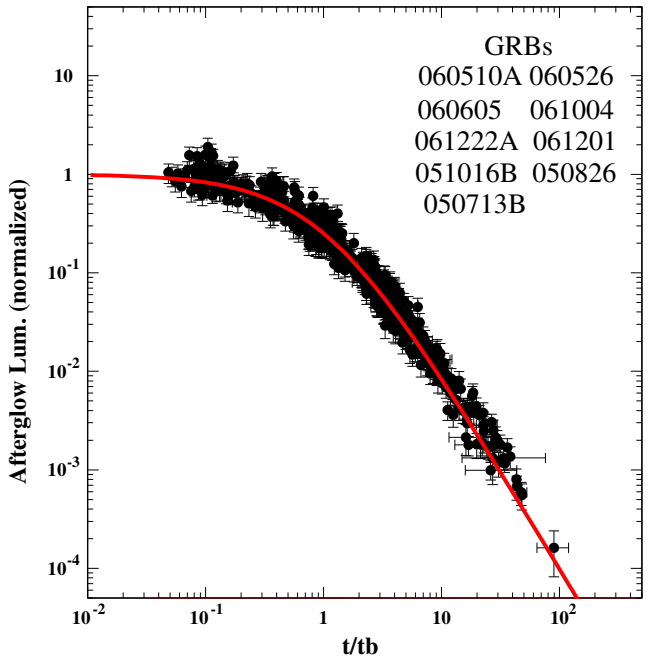

FIG. 6. Comparison between the normalized light curves of well-sampled x-ray afterglows of LGRBs measured with the Swift-XRT [19] in the first couple of days after the burst in the years 2005 and 2006 and their predicted universal behavior as given by Eq. (3). $\chi^2/\text{d.o.f.} = 845/747 = 1.13$.

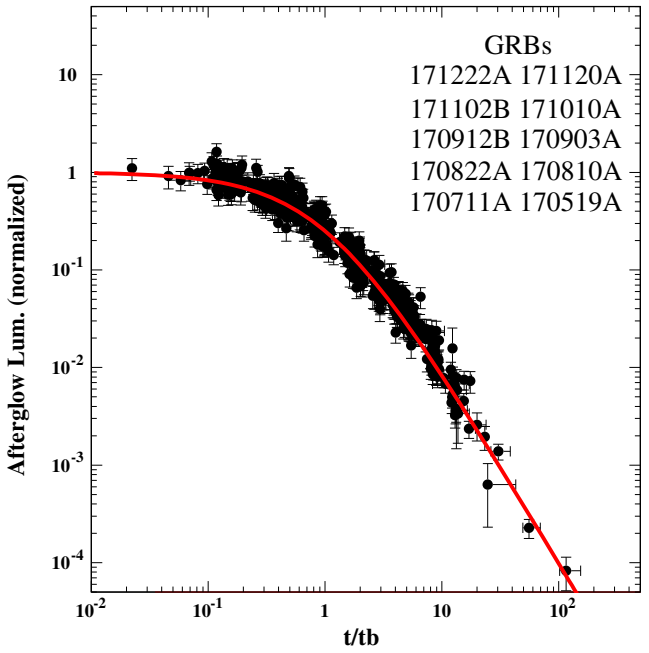

FIG. 8. Comparison between the normalized light curves of well-sampled x-ray afterglows of LGRBs measured with Swift-XRT [19] in the first couple of days after burst in 2017 and their predicted universal behavior as given by Eq. (3). $\chi^2/\text{d.o.f.} = 600/480 = 1.25$.

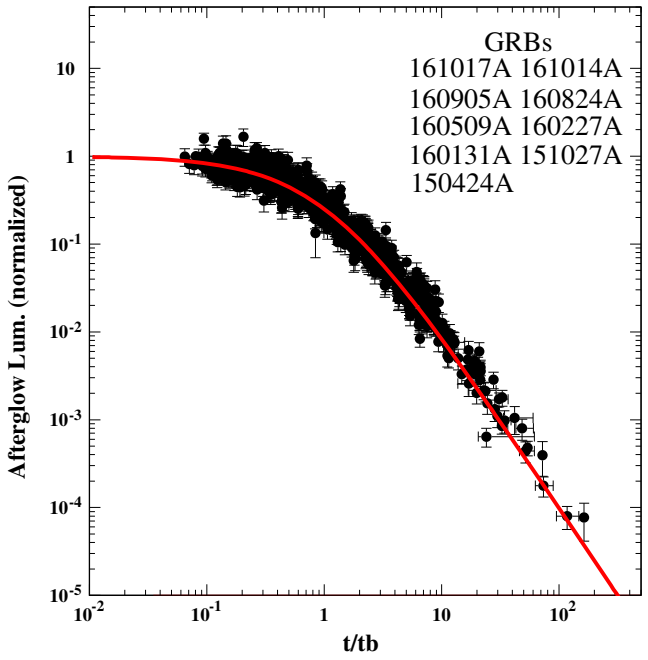

FIG. 7. Comparison between the normalized light curves of well-sampled x-ray afterglows of LGRBs measured with Swift-XRT [19] in the first couple of days after burst in 2015 and 2016 and their predicted universal behavior as given by Eq. (3). $\chi^2/\text{d.o.f.} = 1780/1321 = 1.35$.

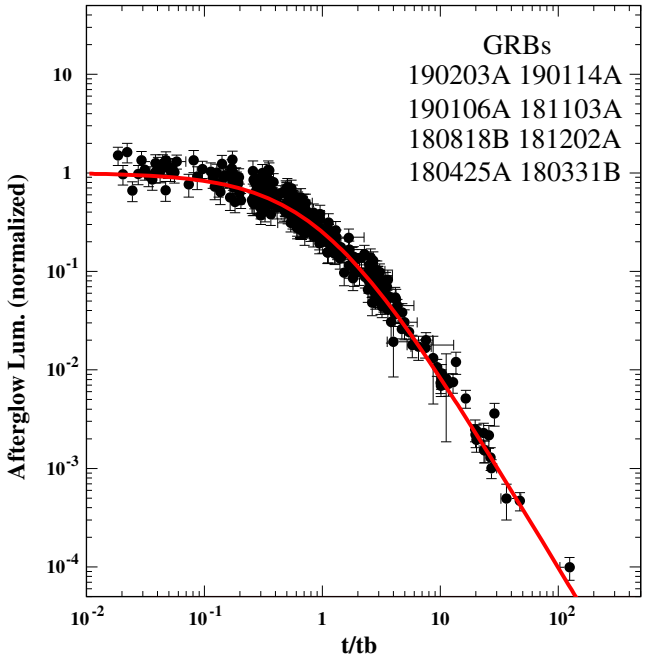

FIG. 9. Comparison between the normalized light curves of well-sampled X-ray afterglow of LGRBs measured with Swift-XRT [19] in the first couple of days after the burst in 2018 and 2019 before May and their predicted universal behavior as given by Eq. (3). $\chi^2/\text{d.o.f.} = 349/343 = 1.02$.

the MINUIT package of the CERN library (wwwasdoc.web.cern.ch/wwwasdoc/minuit/minmain.html). This search program finds the best-fit values of the parameters which minimize the standard χ^2/d.o.f. function defined as $\chi^2 = \Sigma_i(X_i - \mu_i)/\sigma_i^2)$, where X_i are the measured data points with an estimated standard deviation error σ_i, μ_i are the predicted values, d.o.f. is the number of degrees of freedom (the number of data points minus the number of best-fit parameters) and the summation extends over the data points. For each GRB listed in Tables I and II, we have used all the data points reported in Ref. [19] with t values beyond the minimum value where the contribution of the extrapolated fast-decaying prompt emission tail to the afterglow became smaller than the estimated errors reported in Ref. [19] for the plateau data points. The estimated errors in the best-fit values of t_b and $L(0)$ obtained with MINUIT were typically a few percent.

In order to reduce the obscuration of most of the data points by overlying points we have separated the comparison in Fig. 5 into comparisons for individual years, which are shown in Figs. 6–9. For each GRB, all data points with t/t_b larger than the smallest value explained in the text are included in the plots. The value of the χ^2/d.o.f. statistic for all the data points in each year is reported in the caption of each figures. Note in particular that the value of the χ^2/d.o.f. statistic, reported in the captions of Figs. 6–9 has decreased in recent years from 1.35 in 2015–2016 to 1.25 in 2017, and to 1.02 in 2018–2019.

[1] G. J. Fishman and C. A. Meegan, Annu. Rev. Astron. Astrophys. **33**, 415 (1995).

[2] C. A. Meegan, G. J. Fishman, R. B. Wilson, W. S. Paciesas, G. N. Pendleton, J. M. Horack, M. N. Brock, and C. Kouveliotou, Nature (London) **355**, 143 (1992).

[3] R. W. Klebesadel, I. B. Strong, and R. A. Olson, Astrophys. J. **182**, L85 (1973).

[4] J. P. Norris, T. L. Cline, U. D. Desai, and B. J. Teegarden, Nature (London) **308**, 434 (1984); C. Kouveliotou, C. A. Meegan, G. J. Fishman, N. P. Bhat, M. S. Briggs, T. M. Koshut, W. S. Paciesas, and G. N. Pendleton, Astrophys. J. **413**, L101 (1993).

[5] E. Costa, F. Frontera, J. Heise *et al.*, Nature (London) **387**, 783 (1997); J. van Paradijs, P. J. Groot, T. Galama *et al.*, Nature (London) **386**, 686 (1997); M. R. Metzger, S. G. Djorgovski, S. R. Kulkarni, C. C. Steidel, K. L. Adelberger, D. A. Frail, E. Costa, and F. Frontera, Nature (London) **387**, 878 (1997); D. A. Frail, S. R. Kulkarni, L. Nicastro, M. Feroci, and G. B. Taylor, Nature (London) **389**, 261 (1997).

[6] A. Dar, NASA Global Communication Network Circular No. 346 (1999); D. Reichart, Astrophys. J. **521**, L111 (1999); T. J. Galama, N. Tanvir, P. M. Vreeswijk *et al.*, Astrophys. J. **536**, 185 (2000).

[7] E.g., S. E. Woosley, Astron. Astrophys. Suppl. Ser., **97**, 205 (1993); Astrophys. J. **405**, 273 (1993).

[8] S. A. Colgate, CaJPS **46**, 476 (1968); Astrophys. J. **187**, 333 (1974); J. Goodman, A. Dar, and S. Nussinov, Astrophys. J. **314**, L7 (1987).

[9] For the first photometric evidence on SN-GRB associasion see T. J. Galama, P. M. Vreeswijk, J. van Paradijs *et al.*, Nature (London) **395**, 670 (1998); J. S. Bloom, S. R. Kulkarni, S. G. Djorgovski *et al.*, Nature (London) **401**, 453 (1999); For an early review, see A. Dar, arXiv:astro-ph/0405386; For the first spectroscopic evidence see K. Z. Stanek, T. Matheson, and P. Garnavich, Astrophys. J. **591**, L17 (2003); J. Hjorth, J. Sollerman, P. Moller *et al.*, Nature (London) **423**, 847 (2003); For a recent review see, e.g., Z. Cano, S. Wang, Z. Dai, X. D. Zi-Gao, and W. X. Wu, Adv. Astron. **2017**, 1 (2017).

[10] S. Dado, A. Dar, and A. De Rújula, Astron. Astrophys. **388**, 1079 (2002); A. Dar, arXiv:astro-ph/0405386.

[11] A. Gal-Yam, D. Fox, P. Price *et al.*, Nature (London) **444**, 1053 (2006); J. P. U. Fynbo, D. Watson, C. Thone *et al.*, Nature (London) **444**, 1047 (2006); M. Della Valle, Astron Astrophys Trans **29**, 99 (2006); J. Hjorth, J. Sollerman, J. Gorosabel *et al.*, Astrophys. J. **630**, L117 (2005); E. Troja *et al.*, GCN Circular 20222, 2016.

[12] E. Berger, Annu. Rev. Astron. Astrophys. **52**, 43 (2014); W. F. Fong, E. Berger, R. Margutti, and B. A. Zauderer, Astrophys. J. **815**, 102 (2015).

[13] S. I. Blinnikov *et al.*, Sov. Astron. Lett. **10**, 177 (1984); J. Goodman, A. Dar, and S. Nussinov, Astrophys. J. **314**, L7 (1987); Two days before SHB170817A, S. Dado and A. Dar predicted in arXiv:1708.04603 that binary neutron star (BNS) mergers detected by the current LIGO-VIRGO gravitational wave detectors will produce mostly far off axis invisible SGRBs with a universal fast decaying isotropic X-ray afterglow (a "universal" orphan X-ray afterglow).

[14] P. Meszaros and M. J. Rees, Mon. Not. R. Astron. Soc. **257**, 29P (1992).

[15] A. Goldstein, P. Veres, E. Burns *et al.*, Astrophys. J. **848**, L14 (2017).

[16] B. P. Abbott *et al.* (Ligo-Virgo Collaboration) Phys. Rev. Lett. **119**, 161101 (2017); Astrophys. J. **851**, L16 (2017).

[17] Other mechanisms by which newly born MSPs power GRBs and/or their afterglows were proposed, e.g., by E. Blackman and I. Yi, Astrophys. J. **498**, L31 (1998); Z. G. Dai and T. Lu, Phys. Rev. Lett. **81**, 4301 (1998); Astron. Astrophys. **333**, L87 (1998); B. Zhang and P. Meszaros, Astrophys. J. **552**, L35 (2001); Z. G. Dai *et al.*, Science **311**, 1127 (2006); B. D. Metzger, E. Quataert, and T. A. Thompson, Mon. Not. R. Astron. Soc. **385**, 1455 (2008); B. D. Metzger and A. L. Piro, Mon. Not. R. Astron. Soc. **439**, 3916 (2014); B. P. Gompertz, P. T. O'Brien, and G. A. Wynn, Mon. Not. R. Astron. Soc. **438**, 240 (2014); H. Lu, B. Zhang, W. Lei,

Y. Li, and P. D. Lasky, Astrophys. J. **805**, 89 (2015); S. Gibson, G. Wynn, B. Gompertz, and P. O'Brien, Mon. Not. R. Astron. Soc. **470**, 4925 (2017); and references therein.
[18] S. Dado and A. Dar, arXiv:1708.04603; Nuovo Cimento C **41**, 131 (2019).
[19] P. A. Evans *et al.*, Mon. Not. R. Astron. Soc. **397**, 1177 (2009); Astron. Astrophys. **469**, 379 (2007).
[20] M. R. Drout, A. L. Piro, OB. J. Shappee *et al.*, Sci. **358**, 1570 (2017).
[21] E. Pian, P. Soffitta, A. Alessi *et al.*, Astron. Astrophys. **372**, 456 (2001).
[22] F. Harrison, J. S. Bloom, D. A. Frail *et al.*, Astrophys. J. **523**, L121 (1999); G. L. Israel, G. Marconi, S. Covino *et al.*, Astron. Astrophys. **348**, L5 (1999); K. Beuermann, V. F. Hessman, K. Reinsch *et al.*, Astron. Astrophys. **352**, L26 (1999); K. Z. Stanek, P. M. Garnavich, J. Kaluzny, W. Pych, and I. Thompson, Astrophys. J. **522**, L39 (1999).
[23] S. Dado and A. Dar, Astrophys. J. **855**, 88 (2018).
[24] S. Dado, A. Dar, and A. De Rújula, Astrophys. J. **696**, 994 (2009); S. Dado and A. Dar, Astron. Astrophys. **558**, A115 (2013).
[25] S. Dado and A. Dar, Phys. Rev. D **94**, 063007 (2016).
[26] R. N. Manchester and J. H. Taylor, *Pulsars* (W. H. Freeman and Company, San Francisco 1977).
[27] Originally, magnetars were defined to be X-ray pulsars powered by the decay of their ultrastrong magnetic field. Anomalous X-ray pulsars (AXPs) and soft gamma ray repeaters (SGRs), whose observed luminosity was found to exceed their loss of rotational energy [see, e.g., S. Mereghetti, Astron. Astrophys. Rev. **15**, 225 (2008)], were the first discovered pulsars with a luminosity which exceeded their spin down energy release. They were assumed to be powered by the decay of their assumed ultrastrong magnetic field, without a proof. Altenative energy sources, however, such as gravitational energy release by slow contraction or phase transition into a denser form of nuclear matter to become, presumably, strange stars or quark stars (A. Dar and A. De Rújula, Frascati Phys. Ser. **17**, 13 (2000)) were simply ignored.
[28] H. T. Janka, F. Hanke, and L. Hudepohl, Prog. Theor. Exp. Phys. **2012**, 309 (2012).